



Short-term deformation characteristics, displacement prediction, and kinematic mechanism of Baijiabao landslide based on updated monitoring data

Wenmin Yao¹ · Changdong Li^{2,3} · Yuancheng Guo¹ · Robert E. Criss⁴ · Qingjun Zuo⁵ · Hongbin Zhan⁶

Received: 6 July 2021 / Accepted: 27 August 2022 / Published online: 1 September 2022
© Springer-Verlag GmbH Germany, part of Springer Nature 2022

Abstract

Variations of reservoir water level and seasonal precipitation have reactivated or accelerated many reservoir landslides in the Three Gorges Reservoir area since impoundment in 2003. Updated daily monitoring data since 2017 reveals details about the step-like pattern of annual movement of the Baijiabao landslide, a large creeping landslide with a maximal cumulative surface displacement of 0.2 m over this 2-year period. The spatiotemporal deformation characteristics show that mass movement was greatest in 2017 and boundary cracks exhibit more frequent steps and are more sensitive to hydraulic factors than surface displacement. Acceleration periods are triggered when the reservoir water level falls below 153 m above mean sea level, with most annual movement occurring before the reservoir rises back to that critical level. The rate of daily surface movement is controlled by the daily variation of reservoir water level and by cumulative rainfall during the previous 1 to 7 days. The movement responses vary from different years and movement periods, but the one-factor critical-level model can effectively predict surface movement. The correlation between surface displacement rate and reservoir water level also comprehensively indicates the association between landslide movement and hydraulic factors including rainfall and variation of reservoir water level. Low reservoir level and its drawdown, and heavy or continuous rainfall, increase hydraulic gradients and change stress conditions, which destabilize the Baijiabao landslide and accelerate its surface movement.

Keywords Landslide · Controlling factor · Displacement prediction · Kinematic mechanism

Introduction

Landslides in reservoir areas, and particularly in the Three Gorges Reservoir (TGR) area where more than 5000 landslides are recognized, have recently attracted great

attention (Wang et al. 2004; Yi et al. 2011; Paronuzzi et al. 2013; Tomás et al. 2014; Li et al. 2019b; Tang et al. 2019a; Huang et al. 2021). Several catastrophic landslides, including Qianjiangping landslide (Wang et al. 2004), Xintan landslide (He et al. 2010), Shanshucao landslide (Xu et al.

✉ Changdong Li
lichangdong@cug.edu.cn

Wenmin Yao
wmyao@zzu.edu.cn

Yuancheng Guo
guoyc@zzu.edu.cn

Robert E. Criss
criss@wustl.edu

Qingjun Zuo
qjzuo@ctgu.edu.cn

Hongbin Zhan
zhan@geos.tamu.edu

² Faculty of Engineering, China University of Geosciences, Wuhan 430074, China

³ Badong National Observation and Research Station of Geohazards, China University of Geosciences, Wuhan 430074, China

⁴ Department of Earth and Planetary Sciences, Washington University, St. Louis, MO 63130, USA

⁵ National Field Observation and Research Station of Landslides in Three Gorges Reservoir Area of Yangtze River in China, China Three Gorges University, Yichang 443002, China

⁶ Department of Geology & Geophysics, Texas A&M University, College Station, TX 77843-3115, USA

¹ School of Civil Engineering, Zhengzhou University, Zhengzhou 450001, China

2015), Shuping landslide (Wang et al. 2021b), and Kamenziwan landslide (Yin et al. 2020), have occurred since TGR impoundment in 2003, causing many casualties and significant economic loss. Consequently, great efforts have been made to monitor landslides in this area and establish early warning systems.

Among the multi-field information on landslides, surface movement is a key indicator of landslide stability and dynamics and is easy to monitor (Wang et al. 2016; Song et al. 2018; Intrieri et al. 2019; Lacroix et al. 2020; Luo and Huang 2020). Conventional global positioning system (GPS) monitoring networks acquire displacement data on many TGR landslides, typically gathering data one to three times a month (Tomás et al. 2014; Zhang et al. 2020). Such “monthly” data are now available for periods as long as 17 years for several TGR landslides (Tang et al. 2015). Although valuable, “monthly” displacement data have irretrievable drawbacks in evaluating short-term deformation characteristics and evolution mechanisms of landslides. As a result, a few real-time automated multi-field monitoring technologies have been increasingly used so that the short-term behavior of TGR landslides can be studied, but available data and associated research remain limited.

The Baijiabao landslide (Fig. 1) is a large creeping landslide in the TGR area, and monthly GPS data for its deformation are available since 2007. Fortunately, since 2017, daily data have been available on surface movement, crack extension, precipitation, and deep displacement of the sliding zone. The deformation characteristics and controlling factors of the Baijiabao landslide were formerly studied when only the daily monitoring data of about one hydrologic year were available (Yao et al. 2019; Criss et al. 2020). These studies concluded that the landslide experienced a short acceleration period of about 6 weeks, which occurred when the TGR level fell below a critical reservoir water level (RWL) of 153 m above mean sea level (MSL), and that surface movement is controlled by the coupled effect of rainfall and RWL variations. Now that > 2 years of daily monitoring data are available, the short-term deformation characteristics of the Baijiabao landslide can be further studied and prior conclusions tested.

Displacement prediction is an enduringly important topic in landslide research, through which landslide responses to influencing factors and future stability can be learned. Numerous models have been proposed to reach an accurate depiction of the step-like movement of reservoir landslides, which can be normally categorized as empirical models (Van Asch et al. 2009; Bernardie et al. 2015), hydro-mechanical models (Xia et al. 2013; Jian et al. 2014), viscoelastoplasticity models (Desai et al. 1995; Corominas et al. 2005), and computational intelligence

technology-based models (Xu and Niu 2018; Huang et al. 2017; Zhou et al. 2018; Li et al. 2020). Although satisfying prediction performance may be realized, many parameters are generally involved in such models, and some parameters lack sound physical meanings (Liu et al. 2014). The complicated determination of model parameters, over-pretreatment of monitoring data and influencing factors, and high dependency on data quality may limit the applicability of these prediction models (Du et al. 2013). Based on the observed dependence of acceleration on the critical RWL, a parsimonious, one-factor model has been proposed, which captures the timing and step-like movement pattern of the Baijiabao and Shuping landslides (Criss et al. 2020). However, this simple model does not accurately simulate the variable magnitude of annual displacements, suggesting that other factors may also be involved. Understanding the model imperfections can facilitate research on the kinematics of the Baijiabao landslide and similar reservoir landslides.

This study utilizes updated real-time daily monitoring data to investigate the short-term temporal and spatial deformation of the Baijiabao landslide. Controlling factors are identified via the attribution reduction method based on the neighborhood rough set theory. The critical-level model is modified to better predict surface displacement and further its physical meaning, and a conceptual kinematic mechanism for the landslide is then proposed.

Geological setting and monitoring system

The Baijiabao landslide (Fig. 1) is located along the southeast flank of the Zigui Basin, Hubei Province of China (30°58'59.9"N, 110°45'33.4"E). This area has significant topographic relief, with particularly steep slopes near the Yangtze River and its tributaries (i.e., Xiangxi River, Zhaxi River, Qinggan River, and Tongzhuang River). Besides, interbedded Jurassic strata, including sandstone, argillaceous siltstone, mudstone, and soft interlayer from J_{1-2n} (Niejiashan Formation) to J_{3p} (Penglaizhen Formation), are widely distributed (e.g., Li et al. 2017, 2021). These strata are “slide-prone” due to the discrepant geotechnical properties of alternating layers (Yao et al. 2020a, b). The combined effects of stratigraphy, topography, rainfall, and RWL fostered the development of at least 462 landslides in this area, including the Qianjiangping (Wang et al. 2004), Shanshucao (Xu et al. 2015), Shuping (Wu et al. 2018; Criss et al. 2020), and Baijiabao landslides (Fig. 1), which together pose significant threats to residents, transportation, and operation of the Three Gorges Project (Li et al. 2019a).

The elevation of the Baijiabao landslide ranges from 125 to 265 m above MSL, with part of the landslide toe being submerged below reservoir water, whose level has annually

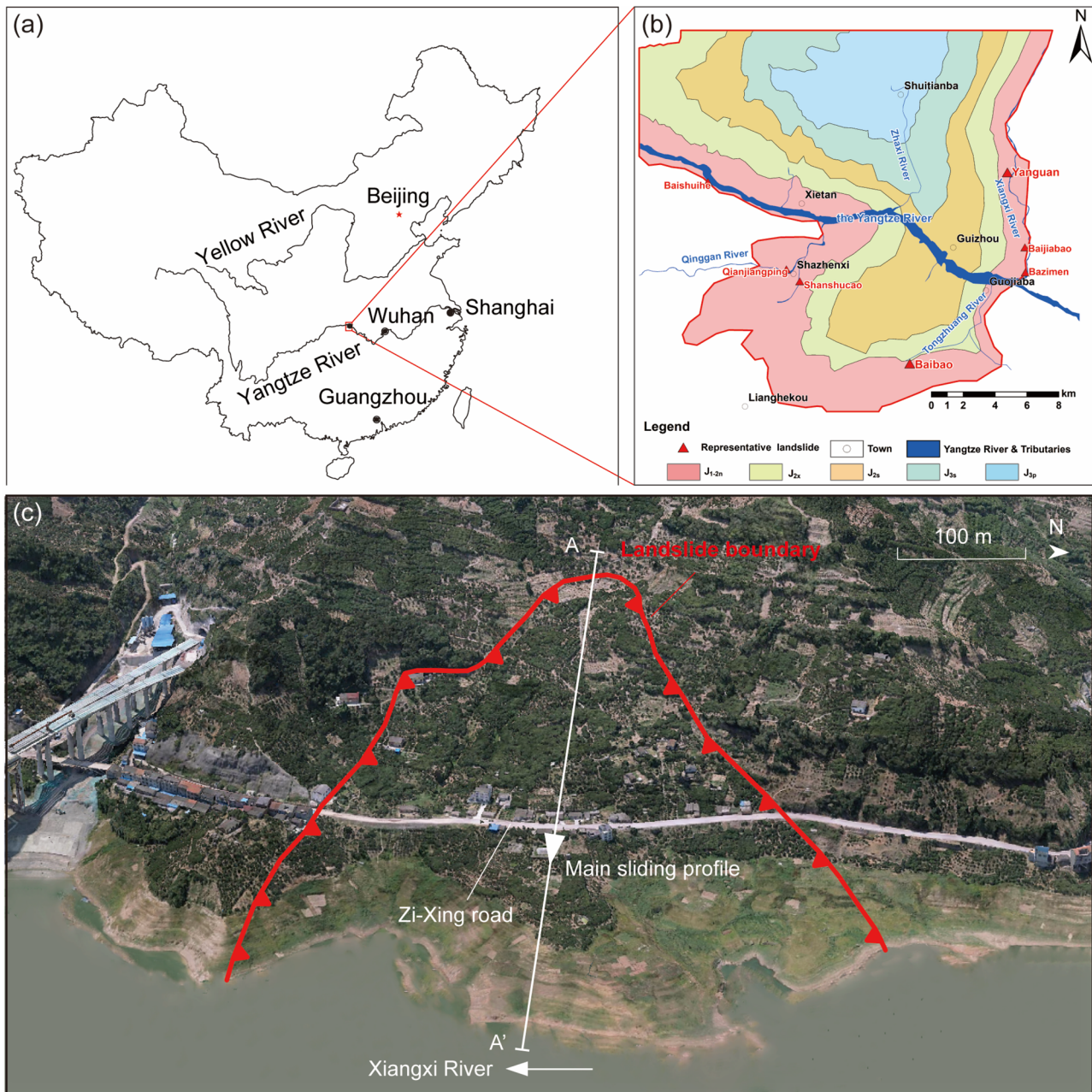


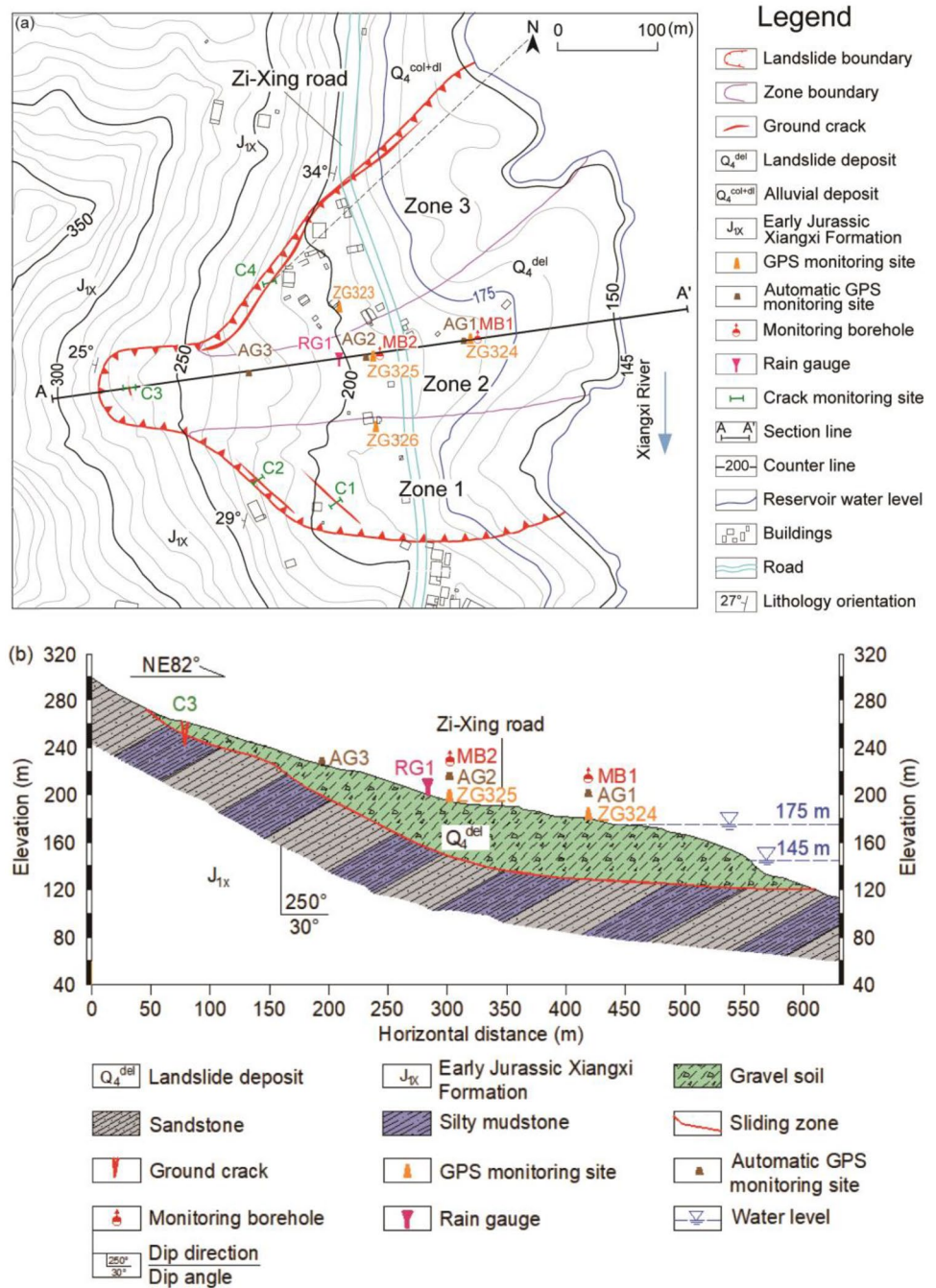
Fig. 1 Location (a, b) and oblique aerial view looking west of the Baijiabao landslide (c), modified after Yao et al. (2019). The arrows in (c) show the flow direction of the Yangtze River and the Xiangxi River

varied from 145 to 175 m above MSL since 2009. The landslide mass is composed of loose Quaternary deposits. The sliding zone of the landslide, with a stair-step shape, is mainly composed of silty clay, while the underlying bedrock contains quartz sandstone and argillaceous siltstone of the Early Jurassic Xiangxi Formation (J_{1x}), which dips into the hill at an angle of 30° to 40° (Fig. 2).

The Baijiabao landslide showed increased creep after TGR impoundment. Systematic monitoring has been performed to capture the deformation characteristics of

the landslide. Briefly, four GPS sites (ZG323-326) were installed in 2006 to monitor the long-term monthly surface movement; and an advanced real-time monitoring network was set up in 2017 to provide high-precision daily monitoring data of rainfall (RM1), surface displacement (AG1–AG3), crack width (C1–C4), and sliding zone displacement (DS1 and DS2) (Fig. 2). Detailed descriptions of geological setting and monitoring system of the Baijiabao landslide have been provided in Yao et al. (2019) and Criss et al. (2020).

Fig. 2 Engineering geological map (a) and geological cross-section (b) of the Baijiabao landslide, modified after Yao et al. (2019). The arrow in (a) shows the flow direction of the Xiangxi River



Short-term deformation characteristics and controlling factors of the Baijiabao landslide

Temporal and spatial deformation process of landslide surface

The Baijiabao landslide was in a state of creep prior to the TGR operation, but the subsequent movement has been

greater and displays a step-like annual movement pattern. Most movement occurs during the rainy season, particularly when precipitation is heavy and RWL is low. During the 13-year GPS monitoring period, the sensor ZG326 recorded the largest cumulative displacement of 1.8 m, and the largest monthly displacement of 244.4 mm (Fig. 3). Following continuous or intense rainfall, anthropogenic activities, and other potentially influencing factors, the landslide moved most rapidly in 2009, 2012, and 2015 (Yao et al. 2019).

During the past 2 years (2018–2019), movements have been smaller than the post-2007 average.

Cumulative displacements of 125.3, 147.4, and 206.4 mm were recorded at AGPS sites AG1, AG2, and AG3 over the 2-year monitoring period (Fig. 4a). The 2019 displacements at these three sites were about 62 to 77% of the 2018 ones. During the 2018 and 2019 rainy seasons, cumulative displacements were > 90% of the two annual totals. Taking AG3 as an example, the displacements in the rainy seasons of 2018 and 2019 were 118.7 and 92 mm, respectively. The daily data of AGPS sites before April 2018 are very noisy, in part because of the new equipment installation and road repair activities, and no significant net movement occurred during this period, so only daily data collected since March 28, 2018, are used below to study the deformation characteristics, controlling factors, and casual rules of landslide acceleration.

During the 32-month period of daily monitoring, the boundary crack sensors C1, C2, and C4 recorded cumulative width extensions of 297.4, 418.3, and 318.4 mm, respectively (Fig. 4b). During the 2018 and 2019 rainy seasons, crack extensions were less than those in 2017. Crack width increased most at C2, with 2017 to 2019 rainy season totals being 113.8, 98.4, and 72.8 mm, respectively.

The terms of acceleration period and rapid movement period are defined to study the movement characteristics of the Baijiabao landslide. Specifically, the acceleration period denotes the continuous time scale corresponding to most displacement in each rainy season; the rapid movement denotes the continuous time scale corresponding to the daily displacement rate greater than 0 during the acceleration period. The daily data show that the landslide surface accelerates

and boundary cracks widen when RWL falls below 153 m above MSL (Criss et al. 2020). The movement rate is greatest when RWL rapidly decreases to the lowest level from 153 m above MSL, and most annual motion occurs before RWL is raised back to 153 m above MSL. The period of rapid movement extended an average of 55 days, from late May to middle-late July (Figs. 4 and 5).

The Baijiabao landslide can be divided into three sub-zones, simply called zone 1, zone 2, and zone 3, based on interval variations in its surface movement (Fig. 2a). The long-term GPS monitoring data and field observations revealed that zone 1 was the most active of the three, with zone 3 being next. As for the short-term daily monitoring data, site AG3 moved faster than the other AGPS sites during the whole monitoring period and individual rainy seasons, and its movement rate varied more than the others. Boundary crack sites C1 and C2 exhibited “one-step” rapid extension during acceleration periods over the monitoring period. However, the width of C2 greatly increased when RWL rose from October to early November 2017 and then widened similarly to C1. Site C4 experienced “multi-step” extensions from October 2017 to February 2018, then showed several pulses of movement during the rainy seasons of 2018 and 2019 (Figs. 4b and 5b). Both temporal differences in different years and movement periods, and spatial differences in various subzones, can be observed from the short-term daily monitoring data. Specifically, the spatial variation of short-term surface movement and crack extension in the three subzones met the long-term GPS data, which could be the result of local geomorphology, strata thickness, depth of sliding zone, ground cracks, drainage condition, etc. (Yao et al. 2019).

Fig. 3 Time-series of “monthly” data on cumulative displacement at four GPS sites, monthly rainfall, and reservoir water level from January 2007 to December 2019

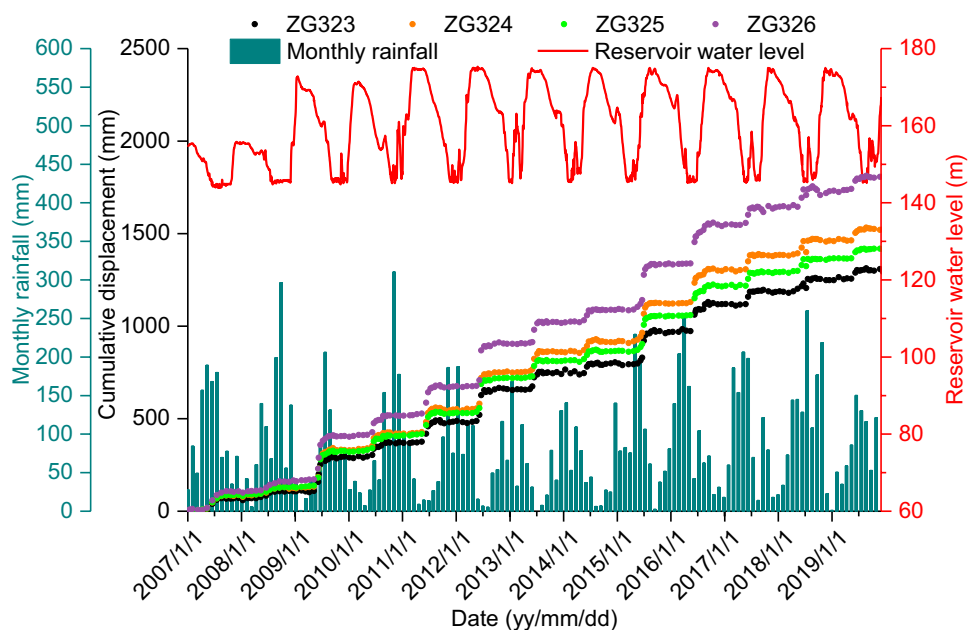
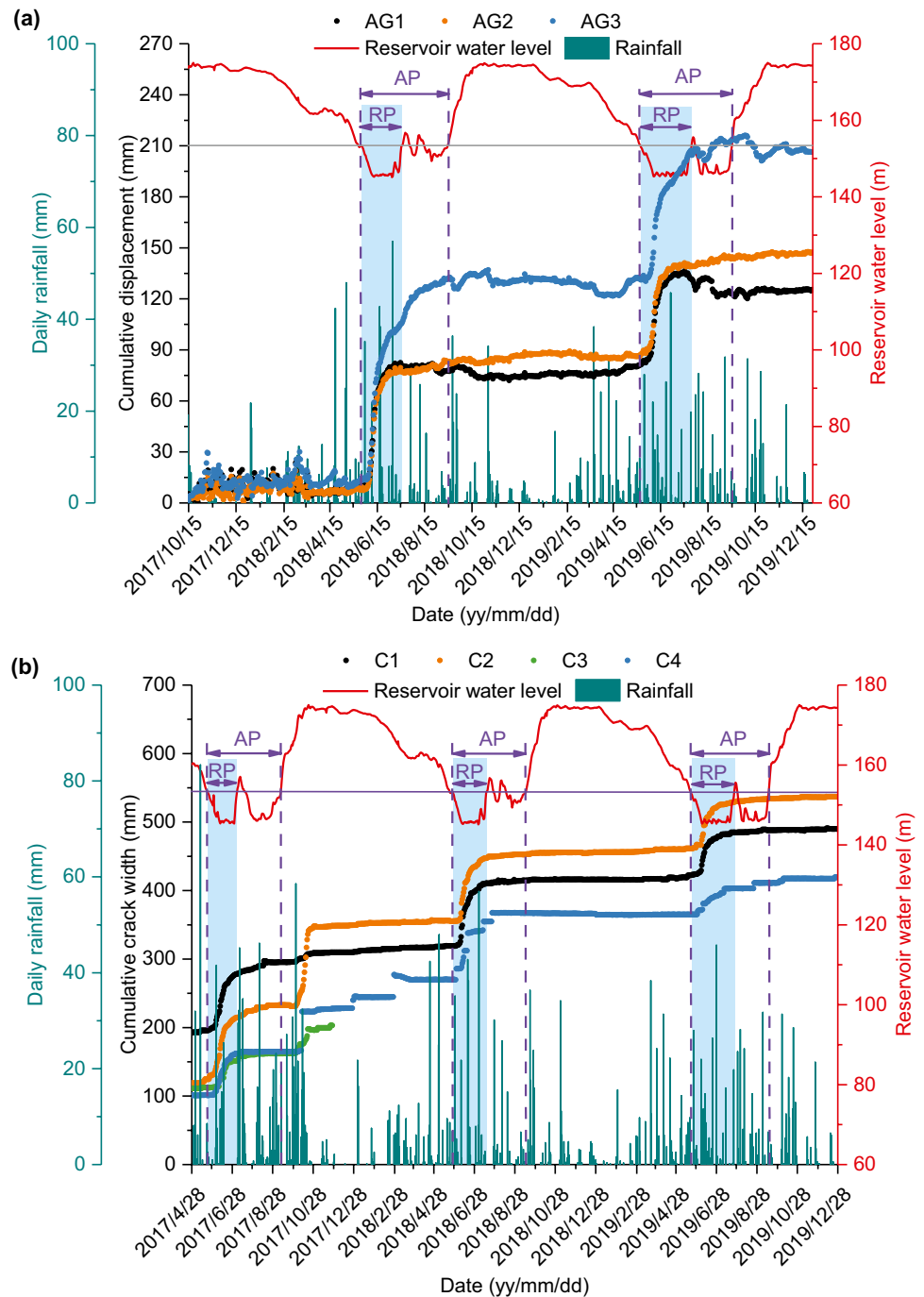


Fig. 4 Time-series of daily data on cumulative displacement of AGPS sites, daily rainfall, and reservoir water level from October 2017 to December 2019 (a); time-series of width of monitored ground cracks, daily rainfall, and reservoir water level from April 2017 to December 2019 (b). RS, rainy season. AP, acceleration period. RP, rapid movement period

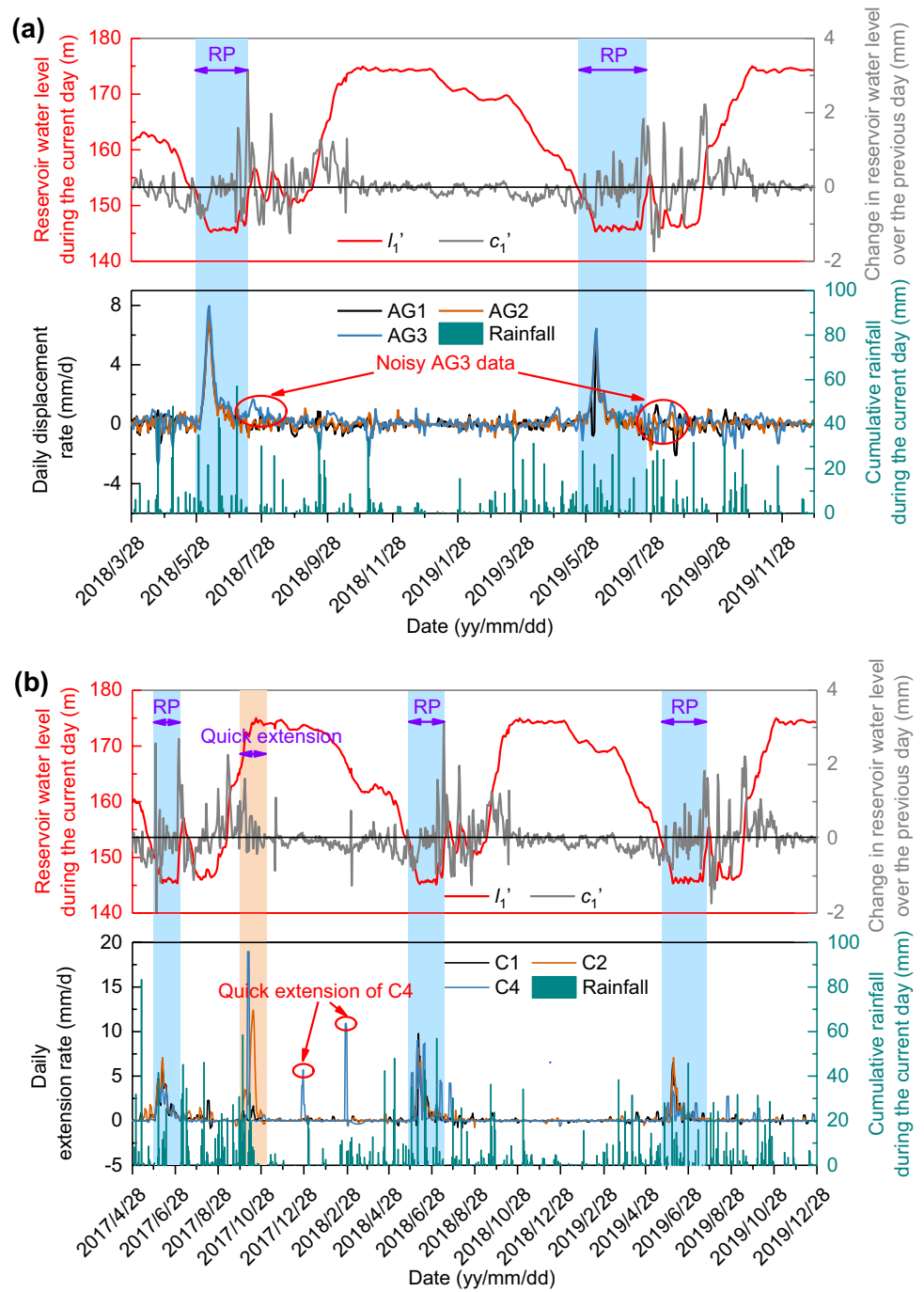


Controlling factors of landslide deformation

The updated monitoring data of the Baijiabao landslide were analyzed using an attribute reduction algorithm, which is based upon neighborhood rough set theory, to identify the controlling factors of the surface deformation. Compared to conventional data mining methods such as a priori algorithms and decision trees, this method can directly deal with numerical and categorical data in attribute reduction

and classification, and can thereby avoid the possible information loss during discretization and clustering using the conventional attribute reduction method (Wilson and Martinez 1997; Hu et al. 2008a, b; Wu et al. 2016; Ma et al. 2017). Through this method, a sub-attribute set that retains the same discriminability as the full attribute set can be obtained for further landslide studies, and the significance of candidate condition attributes to monitoring data can be determined as well.

Fig. 5 Time-dependent variation in daily rates of displacement at AGPS sites from March 2018 to December 2019 (a); time-dependent variation in daily rates of extension of the monitored ground cracks from April 2017 to December 2019 (b). RP, rapid movement period



Consistent with our previous study (Yao et al. 2019), the cumulative rainfall over the previous 2 months was the primary controlling factor of the monthly monitored GPS displacement over the ten potential factors, but during the rainy seasons, the cumulative rainfall during the current month was most important. Several less important factors associated with rainfall and variations of RWL influenced the monthly surface movements (Supplementary Tables S1–S3).

Fourteen potential controlling factors (candidate condition attributes) were evaluated to determine the dominant

ones controlling the short-term daily surface movement of the Baijiabao landslide (Table 1). The significance of these candidate condition attributes to various deformation characteristics are listed in Tables 2 and 3. The change in the RWL over the previous day ($level-change_{1d}$) is the predominant factor controlling the surface movement at the APGS sites, but the cumulative rainfall during the current day ($rainfall_0$) and over different periods (i.e., $rainfall_{1d}$, $rainfall_{7d}$, $rainfall_{15d}$, and $rainfall_{30d}$) also affect the surface movement. Similarly, the width of the monitored boundary cracks

is also most sensitive to level-change_{1d}, but other factors associated with rainfall conditions (rainfall₀, rainfall_{1d}, and rainfall_{7d}) are more important than factors related to longer-term changes in RWL (level-change_{7d}, level-change_{15d}, and level-change_{30d}) and the RWL itself (level₀, level_{1d}, level_{7d}, level_{15d}, and level_{30d}). During rainy seasons, the daily displacement of AGPS sites is most strongly affected by factor level-change_{1d} and cumulative rainfall over the previous 7 days (rainfall_{7d}), while the width of boundary cracks is most sensitive to rainfall₀.

The sensitivities of various hydraulic conditions to monitoring data differ not only among the various data types but among the various monitoring sites and monitoring periods as well. Of the three AGPS sites, AG3 is the most sensitive to factors level-change_{1d} and rainfall₀, and the sensitivities of AG1 and AG 2 to level-change_{1d} and rainfall₀ vary during the whole monitoring period or rainy seasons. Of the boundary crack sites, C1 is the least sensitive to level-change_{1d} and rainfall₀, while C4 is the site most sensitive to rainfall₀ over both the whole monitoring period and rainy seasons.

Causal rules of landslide acceleration

Several critical controlling factors concerning rainfall (rainfall_{7d}), RWL (average RWL during the current day, level₀), and daily variation of RWL (level-change_{1d}) were adopted to study the statistical causal rules of movement acceleration at the AGPS sites (Fig. 6). Rapid surface movement at the AGPS sites mainly occurs when level₀ is between 145 and 153 m, and the reservoir is falling.

Similarly, rainfall₀, level₀, and level-change_{1d} were used to study the causal rules of accelerated extension of crack width (Fig. 7). For C1, rapid extension mainly

occurs when level₀ is between 145 and 153 m above MSL and the reservoir is falling. For C2, rapid extension mainly occurs when (1) level₀ is between 170 and 175 m above MSL, or (2) level₀ is between 145 and 153 m above MSL and the reservoir is falling. Similarly, rapid extension at C4 mainly occurs when level₀ is between 165 and 175 m above MSL, or (2) level₀ is between 145 and 153 m above MSL and the reservoir is falling.

The surface movement at AGPS sites and boundary cracks acceleration is triggered when RWL is below 153 m above MSL, with the drawdown rate of RWL also being a critical factor inducing rapid movement. In contrast, the extension of C2 and C4 is significant when the level of RWL is high, but this is because there was continuous heavy rainfall from October to early November 2017, when the RWL happened to have a high level. Also, the width of C4 experienced “multi-step” extensions when the level of RWL was high (Figs. 4b and 5b).

Displacement prediction of the Baijiabao landslide based on a critical-level model

A critical-level model for the prediction of daily landslide displacement

The updated daily monitoring data of the Baijiabao landslide confirm that the landslide accelerates when the RWL falls below the critical level of 153 m above MSL. A critical-level model has been proposed to predict displacements at GPS and AGPS sites of the Baijiabao landslides (Criss et al. 2020). The model assumes a proportional correlation between the daily displacement rate (dx/dt) of GPS or AGPS sites and the difference between the level₀ (expressed as l_0 in equations) and the critical RWL:

Table 1 Candidate attributes of daily monitoring data concerning surface deformation of the Baijiabao landslide

Candidate condition attributes	Description
Rainfall ₀	The cumulative rainfall during the current day
Rainfall _{1d}	The cumulative rainfall over the previous day
Rainfall _{7d}	The cumulative rainfall over the previous 7 days
Rainfall _{15d}	The cumulative rainfall over the previous 15 days
Rainfall _{30d}	The cumulative rainfall over the previous 30 days
Level ₀	The average reservoir water level during the current day
Level _{1d}	The average reservoir water level over the previous day
Level _{7d}	The average reservoir water level over the previous 7 days
Level _{15d}	The average reservoir water level over the previous 15 days
Level _{30d}	The average reservoir water level over the previous 30 days
Level-change _{1d}	The change in the reservoir water level over the previous day
Level-change _{7d}	The change in the reservoir water level over the previous 7 days
Level-change _{15d}	The change in the reservoir water level over the previous 15 days
Level-change _{30d}	The change in the reservoir water level over the previous 30 days

Table 2 Significance of candidate condition attributes to daily monitoring data concerning surface deformation of the Baijiabao landslide in 1-year and 2-year periods

Monitoring period	Automatic monitoring data	Rainfall ₀	Rainfall _{1d}	Rainfall _{7d}	Rainfall _{15d}	Rainfall _{30d}	Level ₀	Level _{1,d}	Level _{7,d}	Level _{15d}	Level _{30d}	Level-change _{1d}	Level-change _{7d}	Level-change _{15d}	Level-change _{30d}	
2 years	Surface displacement	AG1	0.035	0.021	0.024							0.035			0.010	
		AG2	0.028	0.014	0.027		0.022					0.028				
		AG3	0.057	0.033	0.040	0.031	0.014					0.072	0.022			
	Crack width	C1	0.056	0.043	0.023	0.020	0.014					0.062	0.019			
		C2	0.060	0.039	0.038	0.018	0.014					0.071	0.021			
		C4	0.064	0.042	0.036	0.027	0.018					0.068	0.016			
1 year	Surface displacement	AG1	0.018	0.023								0.032	0.027			
		AG2	0.023				0.027					0.041				
		AG3	0.027		0.036							0.046	0.014			
	Crack width	C1	0.042		0.040	0.017	0.023	0.011				0.074	0.021			0.011
		C2	0.050		0.038	0.025	0.017					0.082	0.042			0.011
		C4	0.048		0.032	0.032	0.025	0.019				0.091	0.034			0.015

Blanks mean that the significance of candidate condition attributes is less than 0.01. Values in bold mean the most important candidate condition attribute to the monitoring sites

Table 3 Significance of candidate condition attributes to daily monitoring data concerning surface deformation of the Baijiabao landslide during rainy seasons

Monitoring period	Automatic monitoring data	Rainfall _{l₀}	Rainfall _{1d}	Rainfall _{7d}	Rainfall _{15d}	Rainfall _{30d}	Level _{l₀}	Level _{7d}	Level _{15d}	Level _{30d}	Level-change _{1d}	Level-change _{7d}	Level-change _{15d}	Level-change _{30d}
2 years	Surface displacement	AG1	0.013	0.020							0.020			
		AG2		0.016							0.026			
		AG3	0.023	0.026	0.033		0.013				0.016			
	Crack width	C1	0.059	0.049	0.022	0.020					0.049	0.022		
		C2	0.059	0.047	0.039	0.022					0.051	0.044		
		C4	0.071	0.049	0.032	0.027					0.064	0.025		
1 year	Surface displacement	AG1	0.013	0.026									0.013	
		AG2	0.013		0.013						0.013			
		AG3	0.026	0.039							0.026	0.033		
	Crack width	C1	0.031	0.035	0.012	0.016					0.063	0.035		
		C2	0.024	0.043	0.024						0.063	0.059		
		C4	0.028	0.028	0.028	0.012	0.024				0.071	0.039		

Blanks mean that the significance of candidate condition attributes is less than 0.01. Values in bold mean the most important candidate condition attribute to the monitoring sites

$$dx/dt = \begin{cases} 0, & \text{for } l_0 \geq 153 \text{ m} \\ k(153 - l_0), & \text{for } l_0 < 153 \text{ m} \end{cases} \quad (1)$$

where k is a scaling factor with units of inverse time. Notably, this model and the following two models can be used to predict and obtain corresponding parameters by linear fitting using the least square method. Although only limited data can be used for linear fitting, further insights into the movement features, evolution processes, and underlying mechanisms may be reached when increasingly monitoring data are available.

The model has been proved as an effective tool for depicting the timing and step-like deformation trend; however, the variable amplitude of the annual steps was not well predicted over the long-term deformation record (Criss et al. 2020). It is confirmed that $level_0$ is associated with landslide acceleration (Fig. 6), but $level-change_{1d}$ and $rainfall_{7d}$ have also been identified as the most important controlling factors of the surface movement at the AGPS sites (Tables 2 and 3). Consequently, two additional models are presented as potential predictive models for the surface movement at AGPS sites of the Baijiabao landslide. The previously proposed critical-level model involving $level_0$ is named the “one-factor” critical-level model. The critical-level model containing factors of $level_0$ and $level-change_{1d}$ is named the “two-factor” model, and that which contains factors of $level_0$, $level-change_{1d}$ (expressed as c_1 in equations), and $rainfall_{7d}$ (expressed as r_7 in equations) is named the “three-factor” model. The explicit formulas of the two-factor and three-factor models are as follows:

$$dx/dt = \begin{cases} 0, & \text{for } l_0 \geq 153 \text{ m} \\ k_1(153 - l_0) + k_2c_1, & \text{for } l_0 < 153 \text{ m} \end{cases} \quad (2)$$

$$dx/dt = \begin{cases} 0, & \text{for } l_0 \geq 153 \text{ m} \\ k_3(153 - l_0) + k_4c_1 + k_5r_7, & \text{for } l_0 < 153 \text{ m} \end{cases} \quad (3)$$

where k_1 and k_2 scaling factors are associated with l_0 and c_1 ; k_3 , k_4 , and k_5 scaling factors are associated with l_0 , c_1 , and r_7 ; all the five coefficients have the unit of day^{-1} . The cumulative displacement can be calculated by adding the predicted daily displacement rate.

During the use of the critical-level model in the prediction of displacement at each AGPS site, when all the monitoring data are directly used, the coefficients are named as fixed k (k in Eq. (1)) in the following parts; when the monitoring data of each year are separately used, the coefficients are named as varied k (k in Eq. (1)), varied 2 k (k_1 and k_2 in Eq. (2)), and varied 3 k (k_3 , k_4 , and k_5 in Eq. (3)); when the monitoring data of each movement periods are separately used, the coefficients are named as varied k' (k in Eq. (1)), varied 2 k' (k_1 and k_2 in Eq. (2)), and varied 3 k' (k_3 , k_4 , and k_5 in Eq. (3)) instead.

Fig. 6 Correlation between daily displacement rates at AGPS sites and the change in the reservoir water level over the previous day, the cumulative rainfall over the previous 7 days, and the average reservoir water level during the current day. **a** AG1, **b** AG2, and **c** AG3

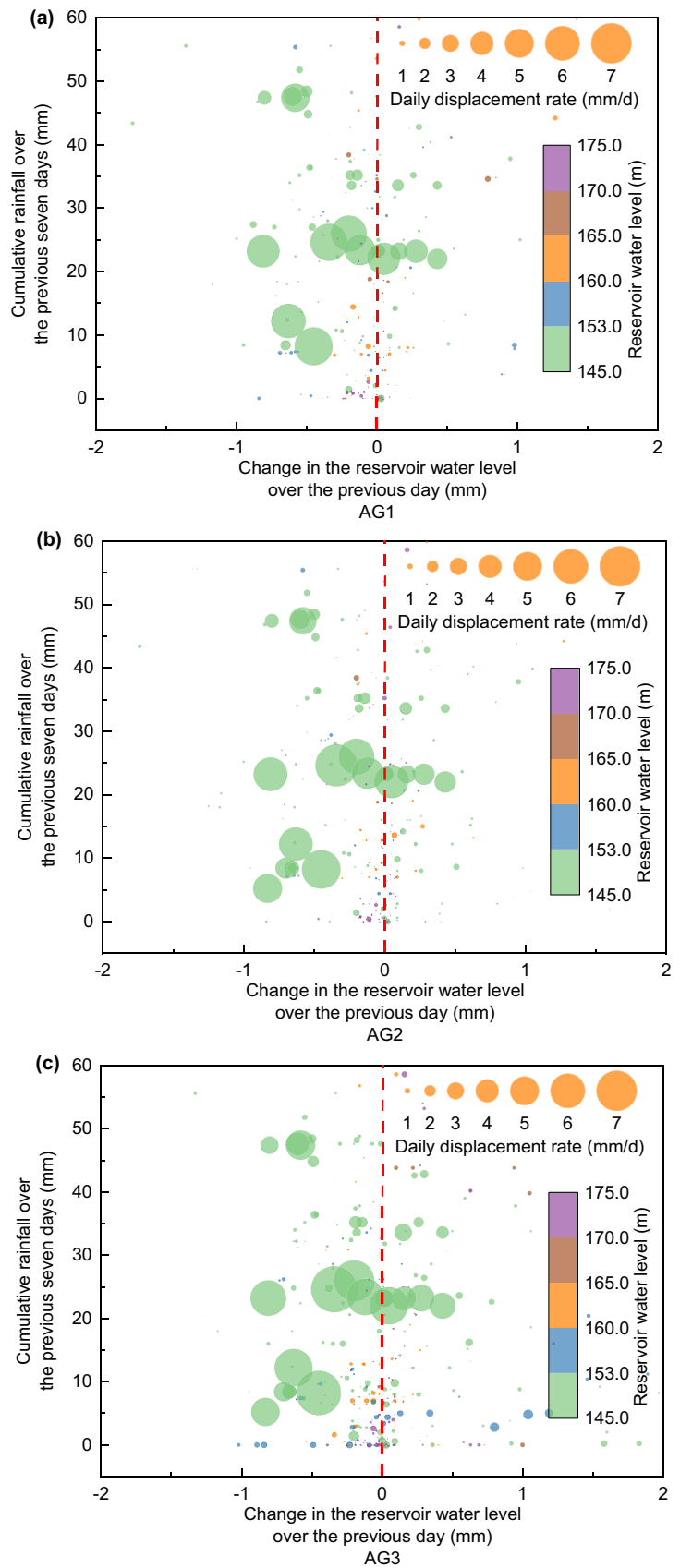
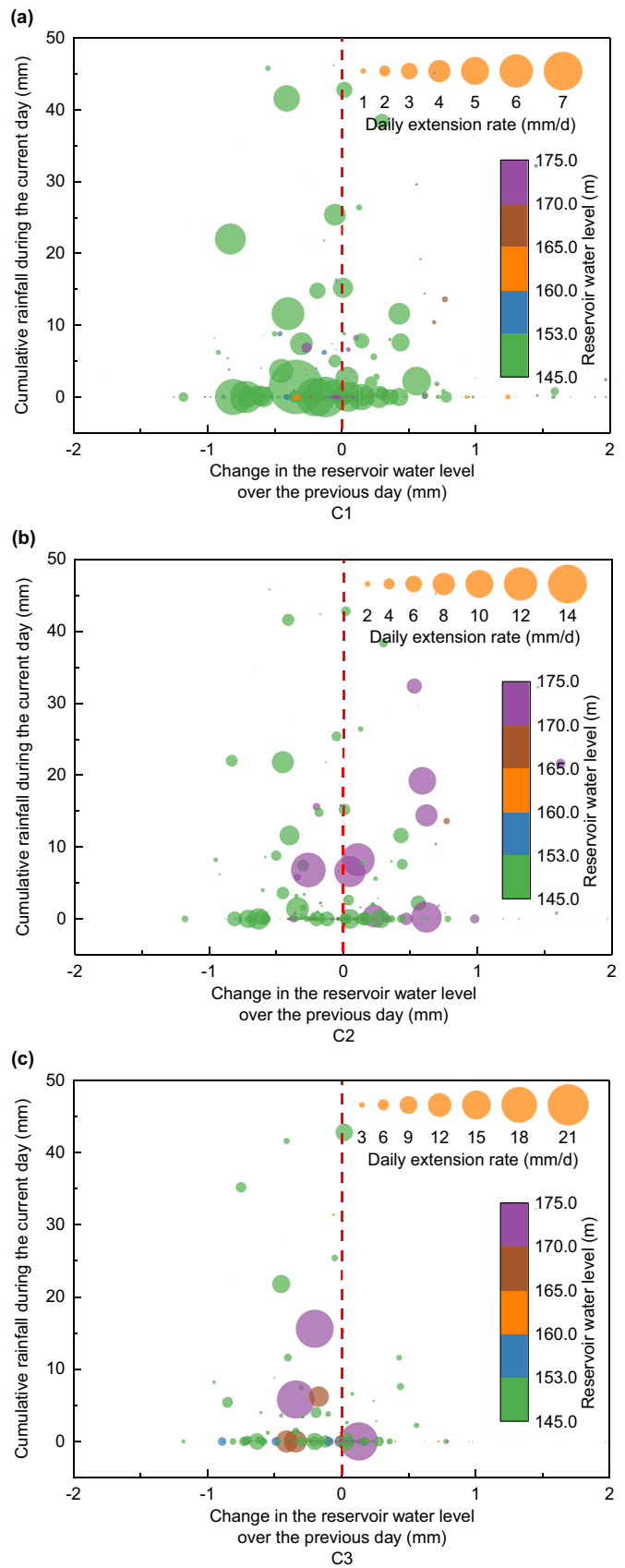


Fig. 7 Correlation between daily extension rates of the monitored cracks and the change in the reservoir water level over the previous day, the cumulative rainfall during the current day, and the average reservoir water level during the current day. **a** C1, **b** C2, and **c** C4



Comparison of critical-level model predictions with short-term daily monitoring data

The original one-factor critical-level model was first used to predict the daily monitoring data at three AGPS sites. When the monitoring data within the 2-year period were used, the prediction results with a fixed k value for each monitoring set were obtained (Fig. 8). The results showed that at the end of the monitoring period, the predicted cumulative displacements of AG2 and AG3 were close to the monitoring data, while the predicted cumulative displacement of AG1 was greater than the monitoring value. For the three AGPS sites, R^2 of 79.52%, 87.50%, and 86.82% can be reached. Specifically, the predicted displacements in 2018 were significantly less than those observed for the actual sites, while the predicted displacements in 2019 are greater than observed. Besides, in addition to the rapid movement periods, periods of slow movement also occurred when RWL was below 153 m above MSL (Fig. 8). The displacement rates of the three AGPS sites did not show significant acceleration but slightly increased or fluctuated during these slow movement periods.

The monitoring data in 2018 and 2019 were then separately analyzed using the one-factor critical-level model. If k values were varied for each year (the monitoring data of each year were separately fitted), the predicted curves met the monitored ones well (Fig. 8). Notably, there were 279 sets of monitoring data in 2018 and 362 sets of monitoring data in 2019 available for the prediction. As the modified critical-level model is an empirical prediction model, all the monitoring data were used to identify the coefficients and compare the responses of the landslide in different years.

The prediction effectiveness, accordingly, was significantly improved (R^2 ranged from 88.11 to 96.68%) (Table 4). The two- and three-factor models were also adopted, whose results were close to those of the one-factor model, and the prediction effectiveness was slightly improved. However, the predicted displacements of AG1 and AG2 were greater than observed, while the opposite was found for AG3.

When the monitoring data during each rapid or slow movement period were separately analyzed using the three models (various k' values), a better agreement between the prediction curves and the monitored ones was secured (Fig. 8; Table 4). The prediction effectiveness was improved with the R^2 up to 94.65%, 97.10%, and 98.36% for AG1, AG2, and AG3, respectively. The surface movement during rapid and slow movement periods can now be well depicted, as there were different deformation responses and characteristics during various movement periods.

Discussion

Physical meaning of critical-level models

The identified crucial controlling factors of the Baijiabao landslide include the daily variation of RWL and antecedent rainfall over intervals of 1 to 7 days. However, no statistically significant rule was found between landslide acceleration and rainfall, while the critical RWL of 153 m is a key trigger of landslide acceleration. The landslide accelerates when RWL is below 153 m above MSL, but RWL was not identified as a rate-controlling factor. Besides, the previously identified important controlling factors were not included in the predictive model as well. The paradox between the movement phenomena and model parameters arises from two aspects: (1) landslide movement is sensitive to RWL only when it is below 153 m above MSL; (2) rainfall can generally promote the movement of landslides, but the landslide is also influenced by RWL and its variation rate; (3) rainfall is an important factor affecting the management of RWL and its rate of change. Thus, the correlation between surface displacement rate and RWL also comprehensively indicates the association between landslide movement and hydraulic factors, including rainfall and RWL variation. Evidence of this hypothesis is that the prediction effectiveness of one- to three-factor models is very close when the k or k' values are varied.

Although the two- and three-factor models appear to have slightly better prediction effectiveness than the one-factor model, this is mostly because more fitting coefficients are involved. Consequently, the one-factor critical-level model is recommended for the prediction and analysis of the surface movement of the Baijiabao landslide on the basis of its simplicity and its dependence only on a single, well-defined variable, the RWL. A fixed value of k can be used to roughly predict the displacement trend in the future, varied k values can be used to predict and analyze the yearly movement of the landslide, and varied k' values can be used to analyze landslide response in different movement periods.

Landslide responses in different years and movement periods

Landslide movements depend on several factors that vary spatially and temporally. If a fixed k value is used in the simple one-factor model, it fails to accurately predict the magnitude of the annual displacements of the Baijiabao landslide. The prediction effectiveness of the one-factor model is significantly improved when k values are varied, indicating that the landslide responses are different each year. Specifically, the landslide responded more strongly to

Fig. 8 Cumulative displacement and prediction results based on critical-level models. **a** AG1, **b** AG2, **c** AG3. For the fixed k case, the k value in the one-factor model is constant for each AGPS site. For the varied k ($2k$, $3k$) cases, the k values in the one-factor (two-factor, three-factor) model vary from each year for each AGPS site. For the varied k' ($2k'$, $3k'$) cases, the k values in the one-factor (two-factor, three-factor) model vary from each movement period for each AGPS site. The curves of varied k and $2k$ in **b** almost overlap, and the curves of varied k , $2k$, and $3k$ in **c** almost overlap as well. RP, rapid movement period. SP, slow movement period

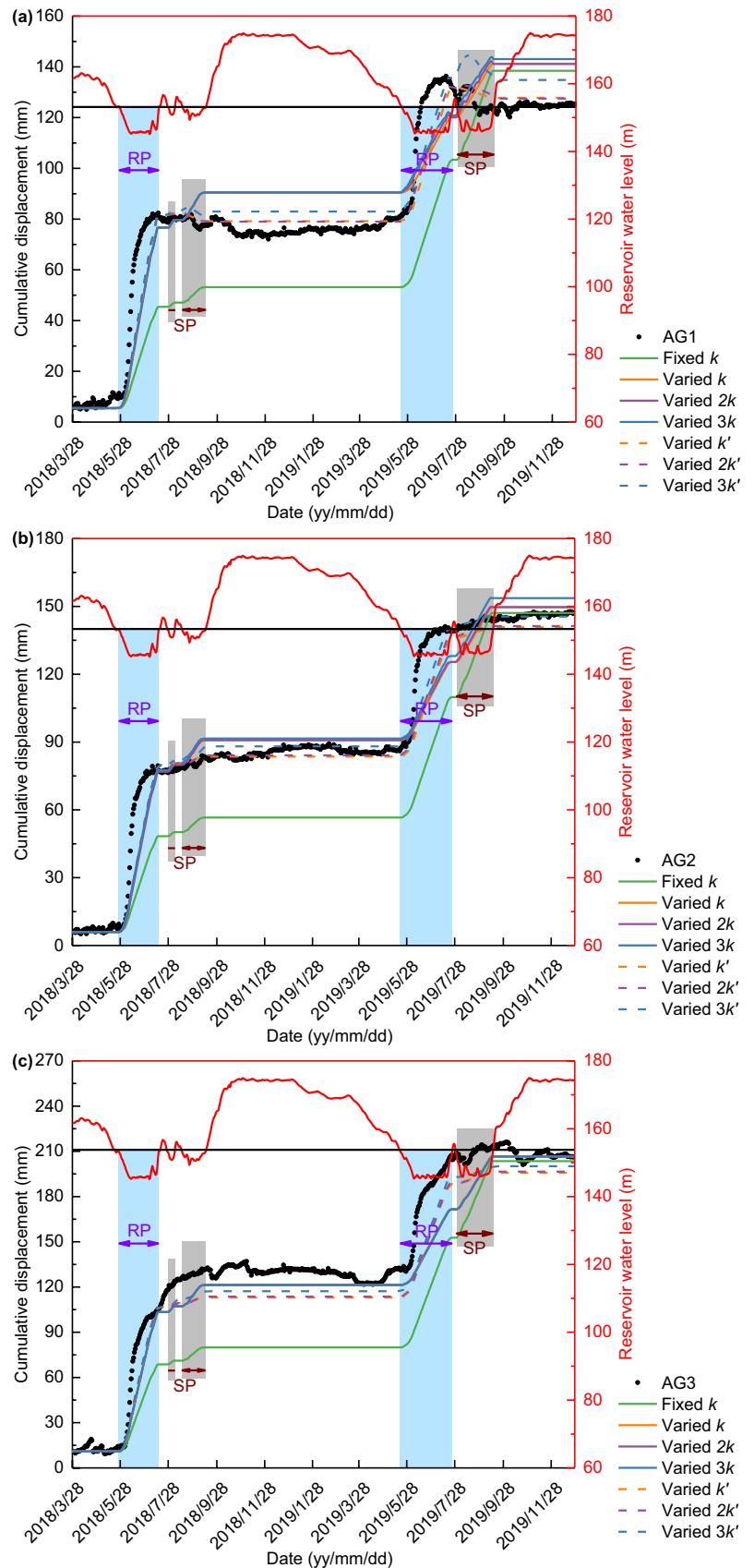


Table 4 Prediction effectiveness of different critical-level models using the daily monitoring data of AGPS sites

AGPS site	Model Variable	One-factor model			Two-factor model		Three-factor model	
		Fixed <i>k</i>	Varied <i>k</i>	Varied <i>k'</i>	Varied 2 <i>k</i>	Varied 2 <i>k'</i>	Varied 3 <i>k</i>	Varied 3 <i>k'</i>
AG1	RMSE (mm)	25.49	14.62	8.48	14.34	7.75	14.66	9.89
	R ² (%)	79.52	88.11	94.65	89.01	95.54	89.38	94.82
AG2	RMSE (mm)	26.64	9.65	8.39	9.57	7.85	9.55	7.01
	R ² (%)	87.50	94.62	97.10	94.72	97.32	95.01	97.18
AG3	RMSE (mm)	42.49	15.27	17.04	15.43	16.48	15.42	13.76
	R ² (%)	86.82	96.68	98.36	96.60	98.44	96.61	98.57

For the fixed *k* case, the *k* value in the one-factor model is constant for each AGPS site. For the varied *k* (2 *k*, 3 *k*) cases, the *k* values in the one-factor (two-factor, three-factor) model vary from each year for each AGPS site. For the varied *k'* (2 *k'*, 3 *k'*) cases, the *k* values in the one-factor (two-factor, three-factor) model vary from each movement period for each AGPS site. *RMSE* root mean squared error, *R*² coefficient of determination

RWL in 2018 than in 2019. Among individual sites, AG3 is the most sensitive site to RWL (Table 5). Also, periods of slow movement followed the rapid movement period in both 2018 and 2019. When variable *k'* values are used in each period, better agreement with observation can be realized (Table 4).

The *k'* values of AGPS sites in each period reveal that AG3 is the most sensitive site to RWL and that AG1 is slightly more sensitive to RWL than AG2 (Table 6). The landslide is more sensitive to RWL in rapid movement periods I and IV in 2018 and 2019, respectively. AG3 is also very sensitive to RWL in period II, followed by periods III and V, while AG1 and AG2 have the sensitivity in the order III > II > V. It should be noted that *k'* values for AG1 in periods III and V are negative; as a result of stress adjustment and strain recovery, the displacement at AG1 fluctuates and tends to decrease in the two periods.

The proposed critical-level model has been validated to be an easy-to-use, accurate, and effective tool for displacement prediction of similar reservoir landslides. Compared to some advanced machine learning models which have satisfying or even greater prediction performance, quick prediction of landslide movement can be made through the proposed model using limited data.

Table 5 Values of fixed *k* and varied *k* in the one-factor critical-level model using the daily monitoring data of AGPS sites

AGPS site	Fixed <i>k</i>	Varied <i>k</i>	
		2018	
		2018	2019
AG1	0.1349	0.2405	0.0803
AG2	0.1431	0.2399	0.0931
AG3	0.1953	0.3125	0.1348

For the fixed *k* case, the *k* value in the one-factor model is constant for each AGPS site. For the varied *k* case, the *k* value in the one-factor model vary from each year for each AGPS site

Kinematic mechanism of the Baijiabao landslide

The kinematic processes of the Baijiabao landslide affected by rainfall and RWL are different. Under intense or continuous rainfall, the rainwater infiltrates into the landslide mass, and a wetting front is formed (Fig. 9). The sliding mass above the wetting front has greater unit weight and weaker strength (e.g., cohesion and friction angle), and the positive pore water pressure increases. The sliding zone near the tailing edge has a small depth and is easy to get saturated as well. The downslope seepage pressure and greater unit weight of the affected shallow sliding mass and sliding zone increase the sliding force of the landslide; the strength degradation of the affected sliding zone decreases the resisting force, destabilizes both the shallow sliding mass and the who landslide (the sliding mass above the sliding zone), thus accelerating the Baijiabao landslide (e.g., rapid surface movement and crack extension). As boundary cracks widen, rainwater can pond in them, and the resultant hydrostatic pressure can further accelerate the crack extension. Besides, when the wetting front moves down to the groundwater level, the groundwater level will uplift, and there will be an increase in sliding force (i.e., increase in gravity) and

Table 6 Values of varied *k'* in the one-factor critical-level model using the daily monitoring data of AGPS sites

AGPS site	Varied <i>k'</i> in 2018			Varied <i>k'</i> in 2019	
	I	II	III	IV	V
AG1	0.2570	0.0539	-0.0680	0.1414	-0.0154
AG2	0.2502	0.0430	0.0660	0.1410	0.0182
AG3	0.3248	0.2026	0.0769	0.2039	0.0267

For the varied *k'* case, the *k* value in the one-factor model vary from each movement period for each AGPS site. I and IV are the rapid movement periods in 2018 and 2019, respectively; II and III are the slow movement periods in 2018, and V is the slow movement period in 2019

Fig. 9 Effect of rainfall on the kinematic process of the Baijiabao landslide. With rainfall infiltration, there is acceleration in the shallow sliding mass and boundary cracks. PWP, positive pore water pressure

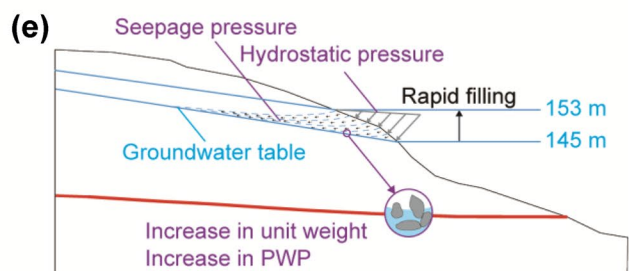
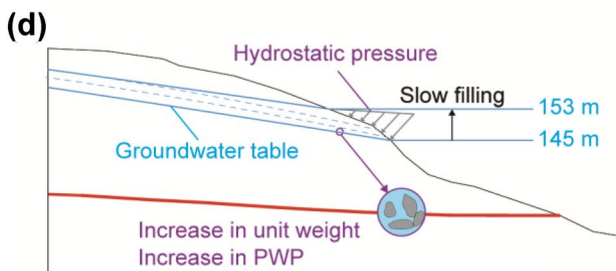
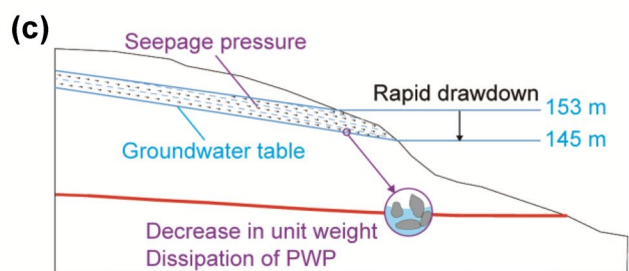
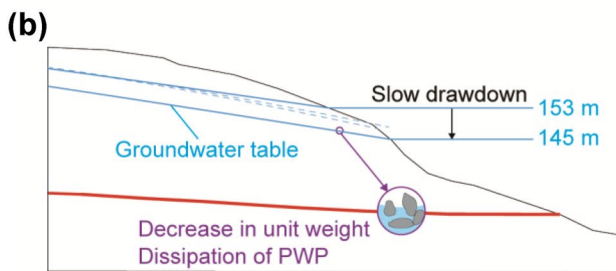
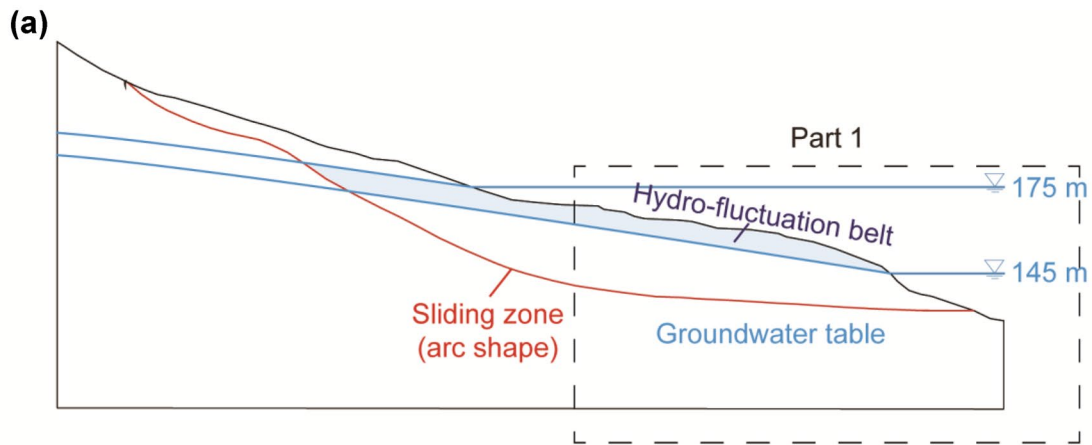
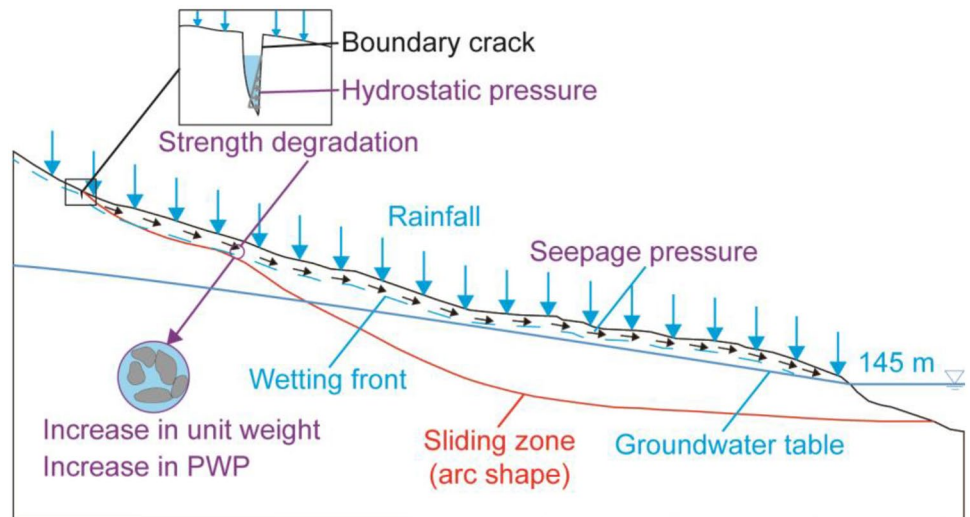
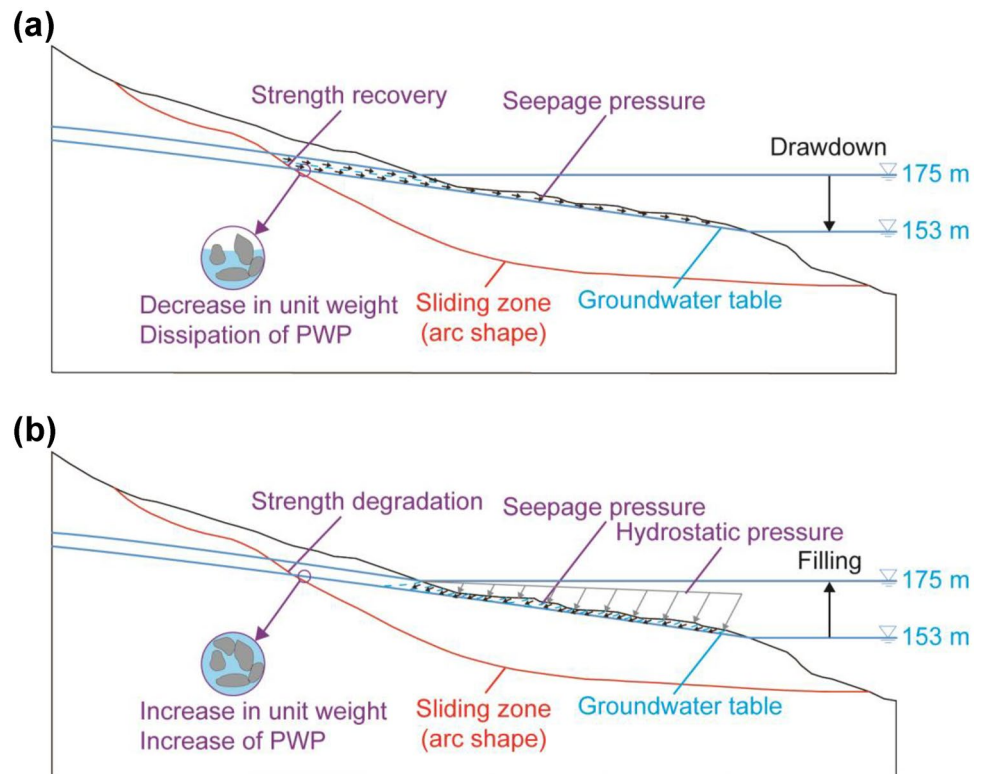


Fig. 10 Effect of reservoir water fluctuation on the kinematic process of the Baijiabao landslide at low level of reservoir water. **a** Sketch illustrating the front part (part 1) influenced by the variations of reser-

voir water level when it is low, **b** slow drawdown, **c** rapid drawdown, **d** slow filling, and **e** rapid filling. The Baijiabao landslide accelerates at low level of reservoir water. PWP, positive pore water pressure

Fig. 11 Effect of reservoir water variations on the kinematic process of the Baijiabao landslide at high level of reservoir water. **a** Drawdown and **b** filling. The Baijiabao landslide remains stable at high level of reservoir water. PWP, positive pore water pressure



a decrease of resisting force (i.e., increase in the gravity of newly affected sliding mass and strength deterioration of newly immersed sliding zone, respectively). Then the stability of the landslide will be decreased and the movement of the landslide will be further accelerated.

When RWL is low (e.g., below 153 m above MSL), the sliding mass in the front part of the Baijiabao landslide (part 1 in Fig. 10) is greatly affected by RWL and its drawdown rate, while the affected sliding zone is in the middle part of the landslide and has a small range. If RWL drawdown is slow, the positive pore water pressure is dissipated synchronously; the unit weight of sliding mass in the hydro-fluctuation belt gradually decreases to the natural value, and the sliding force operating on the Baijiabao landslide decrease (Fig. 10a). In contrast, if the drawdown rate is fast, there will be a decrease in unit weight inadequate dissipation of positive pore water pressure in the area of affected sliding mass, so the downslope seepage pressure is high. In this way, the sliding force of the landslide increases, and the landslide tends to accelerate (Fig. 10b). All the AGPS sites and monitored boundary cracks showed rapid deformation within this scenario. When RWL is rising, there will be an increase in positive pore water pressure, unit weight in the hydro-fluctuation belt, and the hydrostatic pressure on the submerged ground surface. Upslope seepage pressure will also be produced when the rising rate is rapid. Consequently, the sliding force decreases, and surface deformation may cease.

When RWL is high (e.g., higher than 153 m above MSL), the greater part of the sliding mass and sliding zone is affected by variations of reservoir water. The kinematic process of the Baijiabao landslide under reservoir drawdown or filling is similar to that when RWL is low, but there will be strength recovery or degradation of the sliding zone in the meantime, which can greatly affect the stability of the landslide (Fig. 11). Under the coupled effect of changes in the unit weight and positive pore water pressure, strength variation, and seepage pressure, the Baijiabao landslide is in a relatively stable state.

Influenced by topography, stratigraphic units, geotechnical properties, hydrology, RWL, and its variation rate, and other anthropogenic activities (Zangerl et al. 2010; Pinyol et al. 2012; Strauhal et al. 2016; Sun et al. 2016; Wang et al. 2021a; Tang et al. 2019a, b), reservoir landslides can show different responses to variation of RWL. In the TGR area, the Muyubao landslide shows rapid movement when RWL is high, but the filling-drawdown rate has no direct relationship with the deformation of the landslide (Huang et al. 2020). The Shuping landslide accelerates under the critical RWL of 163 m above MSL (Wu et al. 2018; Criss et al. 2020). As for the anaclinal rock slopes in the Wu Gorges, the peak movement velocity occurs at the lowest level of reservoir water (i.e., 145–150 m above MSL) (Huang and Gu 2017). The proposed critical-level model has the potential to capture the first-order movement characteristics and reach a rough prediction of landslide displacement in the future

time based on limited monitoring time and provide insights into the evolution processes and mechanisms of similar reservoir landslides. With sufficient monitoring data available, the uniform response coefficient (k in the prediction model) of each landslide and reach reliable prediction of landslide displacement can also be realized.

Conclusions

The surface movement of the Baijiabao landslide is well documented by 13 years of “monthly” GPS data and > 2 years of daily data. Confirmed by the updated short-term daily monitoring data of landslide movement, the Baijiabao landslide is in a consistent state of intermittent creep with significant temporal and spatial variability. Landslide acceleration is triggered when RWL falls below 153 m above MSL, and most annual movement occurs before RWL is raised back above that critical level.

The daily surface movement of the Baijiabao landslide is mostly affected by the daily change of the reservoir water level and the cumulative rainfall during antecedent periods that range from 1 to 7 days. Because both factors enter into reservoir management, they can be comprehensively reflected by RWL in the one-factor critical-level model. Variable k values in the one-factor level model can improve fitness, indicating that the Baijiabao landslide shows distinct responses to hydraulic factors in different years or movement periods.

The kinematic processes affecting the Baijiabao landslide are controlled by heavy or continuous rainfall, low level of reservoir water, and high reservoir drawdown rate, which can destabilize the Baijiabao landslide and accelerate its surface movement. Recognizing that the critical reservoir water level varies from one reservoir landslide to another, the proposed critical-level model can be used to depict the characteristic movements and trends.

Supplementary Information The online version contains supplementary material available at <https://doi.org/10.1007/s10064-022-02912-8>.

Acknowledgements We sincerely acknowledge the collaborations with the National Field Observation and Research Station of Landslides in Three Gorges Reservoir Area of Yangtze River in China.

Funding This work was supported by the National Natural Science Foundation of China (grant numbers 42107181 and 41922055), the National Key R&D Program of China (grant numbers 2018YFC1507200 and 2017YFC1501304), and the China Postdoctoral Science Foundation (grant number 2021M702932).

Declarations

Competing interests The authors declare no competing interests.

References

- Bernardie S, Desramaut N, Malet JP, Gourlay M, Grandjean G (2015) Prediction of changes in landslide rates induced by rainfall. *Landslides* 12(3):481–494. <https://doi.org/10.1007/s10346-014-0495-8>
- Corominas J, Moya J, Ledesma A, Lloret A, Gili JA (2005) Prediction of ground displacements and velocities from ground-water level changes at the Vallcebre landslide (Eastern Pyrenees, Spain). *Landslides* 2(2):83–96. <https://doi.org/10.1007/s10346-005-0049-1>
- Criss RE, Yao WM, Li CD, Tang HM (2020) A predictive, two-parameter model for the movement of reservoir landslides. *J Earth Sci-China* 31:1051–1757. <https://doi.org/10.1007/s12583-020-1331-9>
- Desai CS, Samtani NC, Vulliet L (1995) Constitutive modeling and analysis of creeping slopes. *J Geotech Eng* 121(1):43–56. [https://doi.org/10.1061/\(asce\)0733-9410\(1995\)121:1\(43\)](https://doi.org/10.1061/(asce)0733-9410(1995)121:1(43))
- Du J, Yin KL, Lacasse S (2013) Displacement prediction in col-luvial landslides, three Gorges reservoir, China. *Landslides* 10(2):203–218. <https://doi.org/10.1007/s10346-012-0326-8>
- He KQ, Wang SQ, Du W, Wang SJ (2010) Dynamic features and effects of rainfall on landslides in the Three Gorges Reservoir region, China: using the Xintan landslide and the large Huangya landslide as the examples. *Environ Earth Sci* 59(6):1267. <https://doi.org/10.1007/s12665-009-0114-5>
- Hu QH, Yu DR, Liu JF, Wu CX (2008a) Neighborhood rough set based heterogeneous feature subset selection. *Inform Sci* 178(18):3577–3594. <https://doi.org/10.1007/s10346-007-0112-1>
- Hu QH, Yu DR, Xie ZX (2008b) Neighborhood Classifiers. *Expert Syst Appl* 34(2):866–876. <https://doi.org/10.1016/j.eswa.2006.10.043>
- Huang D, Gu DM (2017) Influence of filling-drawdown cycles of the Three Gorges reservoir on deformation and failure behaviors of an acinal rock slopes in the Wu Gorge. *Geomorphology* 295:489–506. <https://doi.org/10.1016/j.geomorph.2017.07.028>
- Huang FM, Huang JS, Jiang SH, Zhou CB (2017) Landslide displacement prediction based on multivariate chaotic model and Extreme Learning Machine. *Eng Geol* 218:173–186. <https://doi.org/10.1016/j.enggeo.2017.01.016>
- Huang FM, Tao SY, Huang JS, Fan XM, Jiang SH, Li WB (2021) Efficient and automatic extraction of slope units based on multi-scale segmentation method for landslide assessments. *Landslides* 18:3715–3731. <https://doi.org/10.1007/s10346-021-01756-9>
- Huang XH, Guo F, Deng ML, Yi W, Huang HF (2020) Understanding the deformation mechanism and threshold reservoir level of the floating weight-reducing landslide in the Three Gorges Reservoir Area, China. *Landslides* 17:2879–2894. <https://doi.org/10.1007/s10346-020-01435-1>
- Intrieri E, Carlà T, Gigli G (2019) Forecasting the time of failure of landslides at slope-scale: a literature review. *Earth-Sci Rev* 193:333–349. <https://doi.org/10.1016/j.earscirev.2019.03.019>
- Jian WX, Xu Q, Yang HF, Wang FW (2014) Mechanism and failure process of Qianjiangping landslide in the Three Gorges Reservoir, China. *Environ Earth Sci* 72(8):2999–3013. <https://doi.org/10.1007/s12665-014-3205-x>
- Lacroix P, Handwerger AL, Bièvre G (2020) Life and death of slow-moving landslides. *Nat Rev Earth Environ* 1:404–419. <https://doi.org/10.1038/s43017-020-0072-8>
- Li CD, Wang XY, Tang HM, Lei GP, Yan JF, Zhang YQ (2017) A preliminary study on the location of the stabilizing piles for col-luvial landslides with interbedding hard and soft bedrocks. *Eng Geol* 224:15–28. <https://doi.org/10.1016/j.enggeo.2017.04.020>
- Li CD, Fu ZY, Wang Y, Tang HM, Yan JF, Gong WP, Yao WM, Criss RE (2019a) Susceptibility of reservoir-induced landslides and strategies for increasing the slope stability in the Three Gorges

- Reservoir Area: Zigui Basin as an example. *Eng Geol* 261:105279. <https://doi.org/10.1016/j.enggeo.2019.105279>
- Li CD, Criss RE, Fu ZY, Long JJ, Tan QW (2021) Evolution characteristics and displacement forecasting model of landslides with stair-step sliding surface along the Xiangxi River, three Gorges Reservoir region, China. *Eng Geol* 283:105961. <https://doi.org/10.1016/j.enggeo.2020.105961>
- Li LW, Wu YP, Miao FS, Xue Y, Huang YP (2020) A hybrid interval displacement forecasting model for reservoir colluvial landslides with step-like deformation characteristics considering dynamic switching of deformation states. *Stoch Environ Res Risk Assess* 35:1089–1112. <https://doi.org/10.1007/s00477-020-01914-w>
- Li SL, Xu Q, Tang MG, Iqbal J, Liu J, Zhu X, Liu FZ, Zhu DX (2019b) Characterizing the spatial distribution and fundamental controls of landslides in the three gorges reservoir area, China. *Bull Eng Geol Environ* 78:4275–4290. <https://doi.org/10.1007/s10064-018-1404-5>
- Liu ZB, Shao JF, Xu WY, Chen HJ, Shi C (2014) Comparison on landslide nonlinear displacement analysis and prediction with computational intelligence approaches. *Landslides* 11(5):889–896. <https://doi.org/10.1007/s10346-013-0443-z>
- Luo SL, Huang D (2020) Deformation characteristics and reactivation mechanisms of the Outang ancient landslide in the Three Gorges Reservoir, China. *Bull Eng Geol Environ* 79:3943–3958. <https://doi.org/10.1007/s10064-020-01838-3>
- Ma JW, Tang HM, Liu X, Hu XL, Sun MJ, Song YJ (2017) Establishment of a deformation forecasting model for a step-like landslide based on decision tree C5.0 and two-step cluster algorithms: a case study in the Three Gorges Reservoir area, China. *Landslides* 14(3):1275–1281. <https://doi.org/10.1007/s10346-017-0804-0>
- Paronuzzi P, Rigo E, Bolla A (2013) Influence of filling-drawdown cycles of the Vajont reservoir on MT. *Tec Slope Stability. Geomorphology* 191(5):75–93. <https://doi.org/10.1016/j.geomorph.2013.03.004>
- Pinyol NM, Alonso EE, Corominas J, Moya J (2012) Canelles landslide: modelling rapid drawdown and fast potential sliding. *Landslides* 9(1):33–51. <https://doi.org/10.1007/s10346-011-0264-x>
- Song K, Wang FW, Yi QL, Lu SQ (2018) Landslide deformation behavior influenced by water level variations of the Three Gorges Reservoir (China). *Eng Geol* 247:58–68. <https://doi.org/10.1016/j.enggeo.2018.10.020>
- Strauhal T, Loew S, Holzmann M, Zangerl C (2016) Detailed hydrogeological analysis of a deep-seated rockslide at the Gepatsch reservoir (Klasgarten, Austria). *Hydrogeol J* 24(2):349–371. <https://doi.org/10.1007/s10040-015-1341-3>
- Sun GH, Zheng H, Huang YY, Li CG (2016) Parameter inversion and deformation mechanism of Sanmendong landslide in the Three Gorges Reservoir region under the combined effect of reservoir water level fluctuation and rainfall. *Eng Geol* 205:133–145. <https://doi.org/10.1016/j.enggeo.2015.10.014>
- Tang HM, Li CD, Hu XL, Su AJ, Wang LQ, Wu YP, Criss R, Xiong CR, Li YA (2015) Evolutional characteristics of the Huangtupo landslide based on in situ tunneling and monitoring. *Landslides* 12(3):511–521. <https://doi.org/10.1007/s10346-014-0500-2>
- Tang HM, Wasowski J, Juang CH (2019a) Geohazards in the three Gorges Reservoir Area, China—Lessons learned from decades of research. *Eng Geol* 261:105267. <https://doi.org/10.1016/j.enggeo.2019.105267>
- Tang MG, Xu Q, Yang H, Li SL, Iqbal J, Fu XL, Huang XB, Cheng WM (2019b) Activity law and hydraulics mechanism of landslides with different sliding surface and permeability in the Three Gorges Reservoir Area, China. *Eng Geol* 260:105212. <https://doi.org/10.1016/j.enggeo.2019.105212>
- Tomás R, Li ZH, Liu P, Singleton A, Hoey TB, Cheng X (2014) Spatiotemporal characteristics of the Huangtupo landslide in the Three Gorges region (China) constrained by radar interferometry. *Geophys J Int* 197(1):213–232. <https://doi.org/10.1093/gji/ggu017>
- Van Asch TW, Malet JP, Bogaard TA (2009) The effect of groundwater fluctuations on the velocity pattern of slow-moving landslides. *Nat Hazard Earth Sys* 9(3):739–749. <https://doi.org/10.5194/nhess-9-739-2009>
- Wang FW, Zhang YM, Huo ZT, Matsumoto T, Huang BL (2004) The July 14, 2003 Qianjiangping landslide, three gorges reservoir, China. *Landslides* 1(2):157–162. <https://doi.org/10.1007/s10346-004-0020-6>
- Wang JE, Su AJ, Xiang W, Yeh HF, Xiong CR, Zou ZX, Zhong C, Liu Q (2016) New data and interpretations of the shallow and deep deformation of Huangtupo No. 1 riverside sliding mass during seasonal rainfall and water level fluctuation. *Landslides* 13(4):795–804. <https://doi.org/10.1007/s10346-016-0712-8>
- Wang JE, Schweizer D, Liu QB, Su AJ, Hu XL, Blum P (2021a) Three-dimensional landslide evolution model at the Yangtze River. *Eng Geol* 292:106275. <https://doi.org/10.1016/j.enggeo.2021.106275>
- Wang SM, Pan YC, Wang L, Guo F, Chen YS, Sun WD (2021b) Deformation characteristics, mechanisms, and influencing factors of hydrodynamic pressure landslides in the Three Gorges Reservoir: a case study and model test study. *Bull Eng Geol Environ* 80:3513–3533. <https://doi.org/10.1007/s10064-021-02120-w>
- Wilson DR, Martinez TR (1997) Improved heterogeneous distance functions. *J Artif Intell Res* 11(1):1–34. <https://doi.org/10.1613/jair.346>
- Wu XL, Zhan FB, Zhang KX, Deng QL (2016) Application of a two-step cluster analysis and the Apriori algorithm to classify the deformation states of two typical colluvial landslides in the Three Gorges, China. *Environ Earth Sci* 75(2):146. <https://doi.org/10.1007/s12665-015-5022-2>
- Wu Q, Tang HM, Ma XH, Wu YP, Hu XL, Wang LQ, Criss R, Yuan Y, Xu YJ (2018) Identification of movement characteristics and causal factors of the Shuping landslide based on monitored displacements. *Bull Eng Geol Environ* 78(3):1–14. <https://doi.org/10.1007/s10064-018-1237-2>
- Xia M, Ren G, Ma XL (2013) Deformation and mechanism of landslide influenced by the effects of reservoir water and rainfall, Three Gorges, China. *Nat Hazards* 68(2):467–482. <https://doi.org/10.1007/s11069-013-0634-x>
- Xu GL, Li WN, Yu Z, Ma XH, Yu ZZ (2015) The 2 September 2014 Shanshucao landslide, Three Gorges Reservoir, China. *Landslides* 12(6):1169–1178. <https://doi.org/10.1007/s10346-015-0652-8>
- Xu SL, Niu RQ (2018) Displacement prediction of Baijiabao landslide based on empirical mode decomposition and long short-term memory neural network in Three Gorges area, China. *Comput Geotech* 111:87–96. <https://doi.org/10.1016/j.cageo.2017.10.013>
- Yao WM, Li CD, Zuo QJ, Zhan HB, Criss RE (2019) Spatiotemporal deformation characteristics and triggering factors of Baijiabao landslide in Three Gorges Reservoir region, China. *Geomorphology* 343:34–47. <https://doi.org/10.1016/j.geomorph>
- Yao WM, Li CD, Zhan HB, Zhou JQ, Criss RE, Xiong S, Jiang XH (2020a) Multiscale study of physical and mechanical properties of sandstone in Three Gorges Reservoir region subjected to cyclic wetting-drying of Yangtze River water. *Rock Mech Rock Eng* 53:2215–2231. <https://doi.org/10.1007/s00603-019-02037-7>
- Yao WM, Li CD, Zhan HB, Zhang HW, Chen WQ (2020b) Probabilistic multi-objective optimization for landslide reinforcement with stabilizing piles in Zigui Basin of Three Gorges Reservoir region, China. *Stoch Environ Res Risk A* 34:807–824. <https://doi.org/10.1007/s00477-020-01800-5>
- Yi W, Meng ZP, Yi QL (2011) Theory and method of landslide stability prediction in the Three Gorges Reservoir area. Science Press, Beijing (in Chinese)
- Yin YP, Huang BL, Zhang Q, Yan GQ, Dai ZW (2020) Research on recently occurred reservoir-induced Kamenziwan rockslide in Three Gorges Reservoir, China. *Landslides* 17(8):1935–1949. <https://doi.org/10.1007/s10346-020-01394-7>

- Zangerl C, Eberhardt E, Perzmaier S (2010) Kinematic behaviour and velocity characteristics of a complex deep-seated crystalline rockslide system in relation to its interaction with a dam reservoir. *Eng Geol* 112(1–4):53–67. <https://doi.org/10.1016/j.enggeo.2010.01.001>
- Zhang L, Shi B, Zhang D, Sun YJ, Inyang HI (2020) Kinematics, triggers and mechanism of Majiagou landslide based on FBG real-time monitoring. *Environ Earth Sci* 79:200. <https://doi.org/10.1007/s12665-020-08940-5>
- Zhou C, Yin KL, Cao Y, Intrieri E, Ahmed B, Catani F (2018) Displacement prediction of step-like landslide by applying a novel kernel extreme learning machine method. *Landslides* 15(11):2211–2225. <https://doi.org/10.1007/s10346-018-1022-0>

Springer Nature or its licensor holds exclusive rights to this article under a publishing agreement with the author(s) or other rightsholder(s); author self-archiving of the accepted manuscript version of this article is solely governed by the terms of such publishing agreement and applicable law.